# DiffLoRA: Generating Personalized Low-Rank Adaptation Weights with Diffusion

Yujia Wu<sup>1</sup>, Yiming Shi<sup>1</sup>, Jiwei Wei<sup>1</sup>, Chengwei Sun<sup>1</sup>, Yuyang Zhou<sup>2</sup>, Yang Yang<sup>1</sup>, Heng Tao Shen<sup>1</sup>,

<sup>1</sup>University of Electronic Science and Technology of China <sup>2</sup>Hainan University,

#### **Abstract**

Personalized text-to-image generation has gained significant attention for its capability to generate high-fidelity portraits of specific identities conditioned on user-defined prompts. Existing methods typically involve test-time fine-tuning or instead incorporating an additional pre-trained branch. However, these approaches struggle to simultaneously address the demands of efficiency, identity fidelity, and preserving the model's original generative capabilities. In this paper, we propose DiffLoRA, a novel approach that leverages diffusion models as a hypernetwork to predict personalized lowrank adaptation (LoRA) weights based on the reference images. By integrating these LoRA weights into the text-toimage model, DiffLoRA achieves personalization during inference without further training. Additionally, we propose an identity-oriented LoRA weight construction pipeline to facilitate the training of DiffLoRA. By utilizing the dataset produced by this pipeline, our DiffLoRA consistently generates high-performance and accurate LoRA weights. Extensive evaluations demonstrate the effectiveness of our method. achieving both time efficiency and maintaining identity fidelity throughout the personalization process.

#### Introduction

Recent significant advancements in large-scale text-to-image diffusion models have spurred extensive research into their customizability (Ho, Jain, and Abbeel 2020; Rombach et al. 2022; Song, Meng, and Ermon 2020). A prominent area of emphasis is human-centric customized image generation (Liu et al. 2024; Ruiz et al. 2024; Li et al. 2024; Wang et al. 2024b), which has garnered substantial attention due to its numerous applications, including personalized images with custom styles (Ren et al. 2022; Cui et al. 2024; Zhang et al. 2023), as well as controllable human image generation (Wang et al. 2018; Zhou et al. 2022; Ju et al. 2023). The core idea behind these applications is to integrate user-defined subjects into generated images, enabling users to create personalized visuals consistent with their identity.

To address this demand, various advanced methodologies have been developed for personalization in text-to-image synthesis. One significant approach is model fine-tuning with specific reference images, as outlined in works such

Copyright © 2025, Association for the Advancement of Artificial Intelligence (www.aaai.org). All rights reserved.

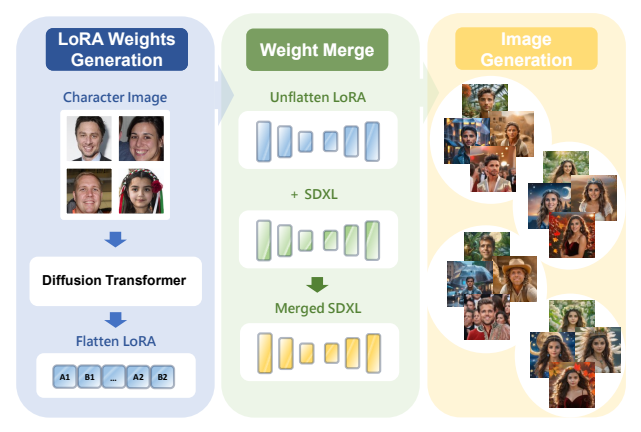


Figure 1: DiffLoRA uses a diffusion transformer model to predict identity-specific LoRA weights from reference images, which are then merged into SDXL for inference.

as (Ruiz et al. 2023; Gal et al. 2023; Kumari et al. 2023; Avrahami et al. 2023; Tewel et al. 2023). These methods can generate high-fidelity images while maintaining the original model's capabilities. However, they require substantial datasets and extensive training, consequently leading to processing times of 10 to 30 minutes per individual personalization, rendering them impractical for user-centric applications. Conversely, studies like (Ye et al. 2023; Wang et al. 2024b; Li et al. 2024; Xiao et al. 2023; Valevski et al. 2023; Wei et al. 2023) achieve personalization without test-time fine-tuning by incorporating an additional trainable condition branch. While these tuning-free methods provide a viable alternative, they often compromise the model's fidelity and versatility, struggling with maintaining identity fidelity and the original generative capabilities of the model (Zeng et al. 2024). Moreover, freezing the original diffusion model's weights to train an auxiliary learnable branch also incurs extra training cost and increases inference cost compared to the original diffusion model (Ju et al. 2023).

Inspired by the success of low-rank adaptation (LoRA) (Hu et al. 2022) and hypernetworks (Peebles et al. 2022; Ha, Dai, and Le 2022), we propose a novel latent diffusion-based hypernetwork framework, named DiffLoRA, designed to predict the LoRA weights. Unlike previous approaches that use hypernetworks to generate weights of specific compo-

nents such as multilayer perceptron (MLP) or normalization layers (Erkoç et al. 2023; Wang et al. 2024a), our framework provides a comprehensive solution for generating the LoRA weights of specific identity, guided by the reference image conditions, as illustrated in Figure 1. DiffLoRA contains contains an autoencoder for LoRA weights and a diffusion transformer model specifically tailored for LoRA. This framework synthesizes facial and overall mixed feature information of reference images utilizing a Mixtureof-Experts-inspired (MoE-inspired) gate network (Shazeer et al. 2016). During the inference phase, the diffusion model leverages these mixed features as conditional inputs to facilitate the denoising process. By reconstructing LoRA latent representations with the decoder, we can obtain the corresponding LoRA weights for specific identity adaptation in the Stable Diffusion XL (SDXL) model (Podell et al. 2023). Such a latent diffusion-based hypernetwork framework enables the prediction of a larger scale of parameters compared to other frameworks (Wang et al. 2024a). Additionally, the diffusion framework supports cross-modality generation, achieving more stable and superior results compared to other network frameworks through iterative denoising (Ruan et al. 2023; Zhang et al. 2024). By merging the LoRA weights generated by DiffLoRA into the SDXL, the model achieves personalization without additional fine-tuning, while maintaining identity consistency and preserving the original generative capabilities without introducing additional inference cost.

Our DiffLoRA framework necessitates LoRA weights for multiple identities during training, thereby requiring the support of a specialized LoRA weight dataset. However, there is currently no standard dataset available for LoRA weights of specific identities. To address this gap, we have developed an automated pipeline to construct a LoRA weight dataset tailored for various identities, to facilitate the training of DiffLoRA. This pipeline generates a high-quality LoRA weight dataset by processing images of each identity with diverse expressions, attributes, and scenes, utilizing techniques such as DreamBooth (Ruiz et al. 2023) for model training.

To summarize, the main contributions of our work include:

- To the best of our knowledge, we make the first attempt to leverage diffusion models guided by reference images to generate LoRA weights for personalized image generation. This tuning-free method enables the generation of high-fidelity personalized portraits without additional computational cost during inference.
- We propose a specialized LoRA weight autoencoder for LoRA weights compression and reconstruction. Additionally, we introduce a MOE-inspired gate network that dynamically integrates detailed facial features and general image features for enhanced identity extraction.
- We introduce a new data pipeline for constructing the LoRA weight dataset, which facilitates DiffLoRA training and ensures the representation of a diverse range of identities.
- Comprehensive experiments show that our method significantly outperforms existing state-of-the-art ap-

proaches in text-image consistency, identity fidelity, generation quality, and inference cost.

### **Related Work**

#### **Personalization in Diffusion Models**

Personalized image generation using diffusion models has gained significant attention in recent research. Diffusion models (Nichol and Dhariwal 2021; Saharia et al. 2022; Ramesh et al. 2022) use pre-trained text encoders like CLIP (Radford et al. 2021) to encode text prompts into latent space. Stable Diffusion (Rombach et al. 2022) and its advanced version, SDXL (Podell et al. 2023), improve computational efficiency and image quality with enhanced architectures. Early personalization methods, like DreamBooth (Ruiz et al. 2023) and Textual Inversion (Gal et al. 2023), require extensive fine-tuning for each subject. Recent techniques offer tuning-free personalization by adding branches to inject identity information during inference (Wang et al. 2024b; Li et al. 2024; Wei et al. 2023). Our DiffLoRA approach, predicts and loads LoRA weights from a reference image into the SDXL, eliminating retraining. Since LoRA is a general fine-tuning method, DiffLoRA can integrate into existing Parameter-Efficient Fine-Tuning (PEFT) methods, enabling flexible applications across various tasks.

#### **Parameter Generation**

Parameter Generation, known as predicting model parameters through hypernetworks (Ha, Dai, and Le 2022), has seen significant advancements. Hypernetworks dynamically generate model weights, offering flexibility and efficiency. Recently, diffusion models have been employed as hypernetwork frameworks, resulting in more stable and superior outcomes. For instance, (Zhang et al. 2024; Erkoç et al. 2023; Peebles et al. 2022) demonstrate that diffusion models as hypernetworks yield better results compared to other frameworks. These methods leverage the strengths of diffusion models to predict network weights. Furthermore, the scalability of this approach allows for seamless integration with other techniques, making it highly suitable for personalized image generation (Ruiz et al. 2024). In our research, we examine the advantages of LoRA relative to MLP and subsequently design a novel diffusion model framework to align with target LoRA weights.

## **Preliminaries and Motivation**

This section establishes the foundational concepts and motivations underpinning our research. **Section Preliminaries** explores the core principles of Latent Diffusion Models (Rombach et al. 2022), which form the cornerstone of our proposed methodology. **Section Motivation** presents a comprehensive analysis of why LoRA weights offer greater efficiency and ease of fitting relative to MLP weights.

### **Preliminaries - Latent Diffusion Models**

LDMs are diffusion models operating on latent representations instead of original samples. Images are projected into latent representations by a VAE (Kingma and Welling 2013; Razavi, Van den Oord, and Vinyals 2019). The diffusion process occurs on these latent representations, guided by conditions for step-by-step denoising. The objective is to minimize the discrepancy between the predicted noise and the actual noise injected at each timestep, using a loss function similar to those in vanilla diffusion models (Ho, Jain, and Abbeel 2020; Song, Meng, and Ermon 2020; Sohl-Dickstein et al. 2015), formulated as:

$$L_{LDM} = \mathbb{E}_{t,z,\epsilon} \left[ \left\| \epsilon - \epsilon_{\theta} \left( \sqrt{\bar{\alpha_t}} z_0 + \sqrt{1 - \bar{\alpha_t}} \epsilon, c, t \right) \right\|^2 \right], \quad (1)$$

where  $z_0$  is the latent representation of a training sample  $x_0$ ,  $\epsilon$  is the actual noise, and  $\epsilon_\theta$  is the model's noise estimate at timestep t. Here, c denotes condition embeddings, and  $\bar{\alpha}_t$  is a variance-preserving coefficient. By incorporating condition-guided embeddings, the model can produce diverse and contextually relevant latent representations, which are essential for various downstream tasks.

## **Motivation - Why Predict LoRA Weights?**

In this section, we provide a detailed theoretical analysis of why LoRA weights are easier to predict relative to MLP weights. We argue that the efficiency of low-rank structures and their constrained distribution range contribute significantly to this advantage.

Low-rank adaptation (LoRA) significantly reduces the required parameter count through its low-rank structures. For an  $m \times n$  matrix, LoRA stores two smaller matrices, resulting in a total parameter count of  $(m+n) \times r$ , where r is the low-rank factor. This reduction in parameters lowers computational complexity during optimization, thereby enhancing training efficiency. Mathematically, the low-rank approximation constrains the parameter space, reducing the degrees of freedom from mn to (m+n)r, where  $r \ll$  $\min(m, n)$ . Additionally, the constrained distribution range of LoRA weights facilitates their compression and reconstruction. This more concentrated and stable parameter distribution improves generalization by reducing the risk of overfitting (Biderman et al. 2024). This inherent characteristic of LoRA makes it more efficient relative to full-rank MLP weights, enabling better performance with fewer computational resources.

To better demonstrate our theoretical claims, we design a toy experiment focusing on the compression and reconstruction of low-rank features. Following the methodology outlined by (Prasantha, Shashidhara, and Murthy 2007) for image compression using Singular Value Decomposition (SVD) (Klema and Laub 1980), we perform SVD on several face images from the FFHQ dataset (Karras, Laine, and Aila 2019) and extract the low-rank matrices of the top few dimensions to obtain the low-rank features. This method leverages SVD's ability to compact energy effectively and capture local statistical variations, resulting in efficient compression into low-rank features (Guo et al. 2015).

Subsequently, we train two autoencoders with identical parameters to reconstruct full-rank and low-rank features, respectively. During training, both autoencoders aim to reconstruct the original images. In the testing phase, we com-

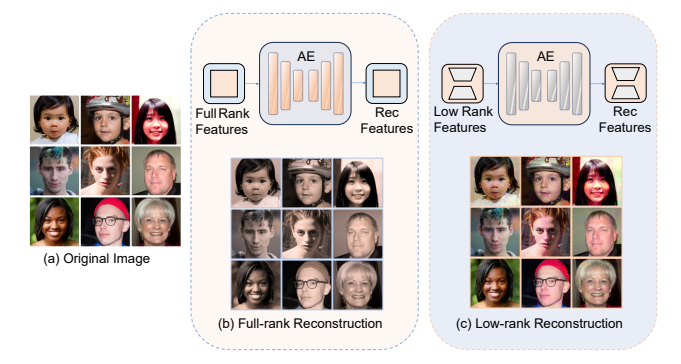


Figure 2: A toy experiment to demonstrate the low-rank features are easier to compress and reconstruct. Two autoencoders with identical parameters are trained to reconstruct full-rank and low-rank features, respectively. In testing, the low-rank features enable the autoencoder to achieve superior reconstruction quality with the same configurations.

pare the reconstruction quality of the images by peak signal-to-noise ratio (PSNR) and structural similarity index (SSIM) metrics (Hore and Ziou 2010). The results, as shown in Figure 2, indicate that the autoencoder reconstructing the low-rank features achieves higher PSNR and SSIM values, suggesting superior reconstruction quality with the same computational cost.

This empirical evidence supports our hypothesis that lowrank features are easier to compress and reconstruct, and by extension, LoRA weights are more efficient to predict.

#### Method

## **LoRA Weights Generation**

Given reference images, DiffLoRA aims to efficiently generate accurate LoRA weights by leveraging a LoRA weight autoencoder (LAE) combined with a diffusion model. This approach circumvents the extra training cost associated with dual-branch architectures while achieving high-fidelity image generation through LoRA weight generation and weight merging. We begin by detailing the construction of the LAE to compress LoRA weights into a latent space. Next, following (Erkoç et al. 2023), we describe our diffusion transformer (DiT) model training to directly predict encoded LoRA latent representations, rather than the noise. We then introduce the Mixed Image Features (MIF) mechanism to integrate face features and image features from images, guiding the DiT model in the denoising process. Lastly, we outline the dataset construction pipeline for generating LoRA weights that accommodate multiple identities. Figure 3 provides an overview of our training and inference process.

#### LoRA Weight Autoencoder

As shown in Figure 3, the LoRA weight autoencoder (LAE) is designed to effectively compress and reconstruct the LoRA, specifically targeting the structural and informational correlations inherent in LoRA.

As for the structural feature, unlike images, the shapes of LoRA weights are not identical, with LoRA-A having a shape of  $\mathbb{R}^{n\times n}$  and LoRA-B having a shape of  $\mathbb{R}^{m\times r}$ , ne-

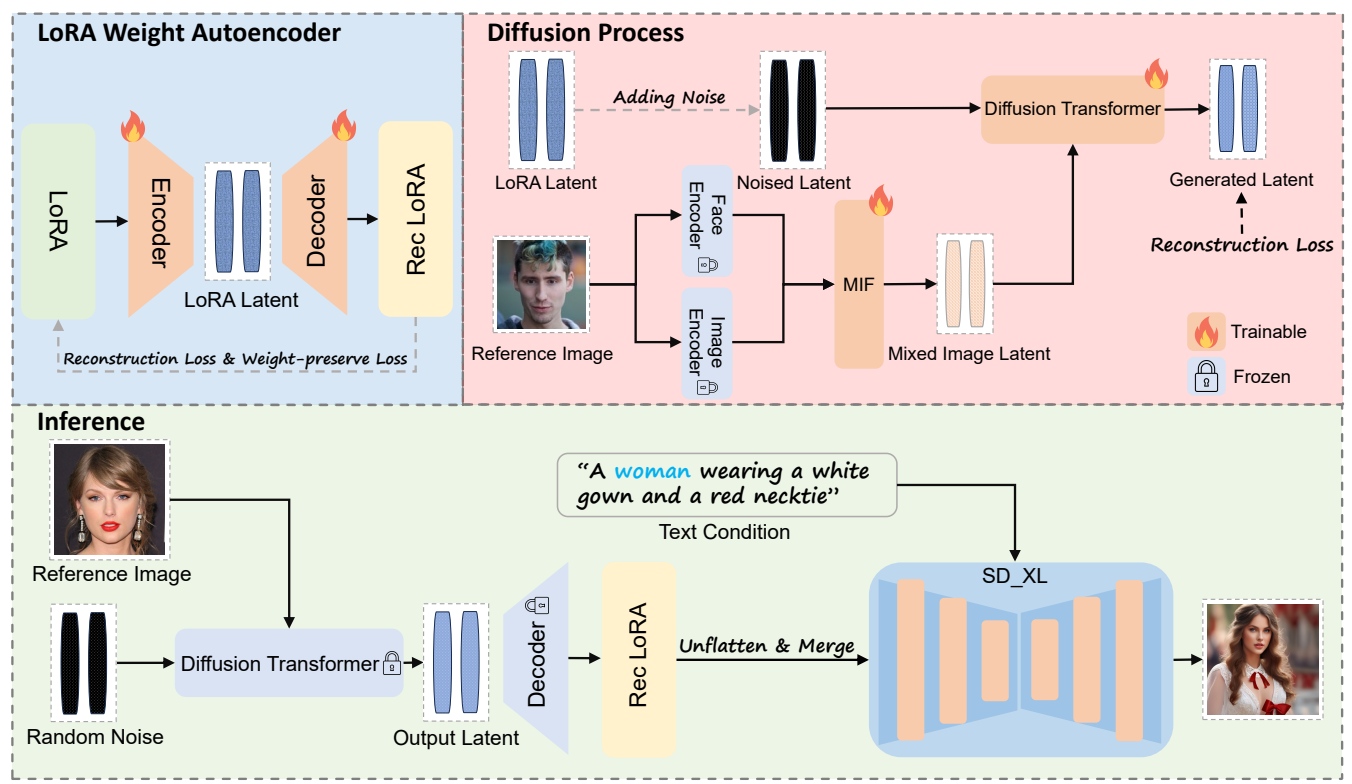


Figure 3: Overview of DiffLoRA. Our approach consists of two stages: LoRA weight autoencoder (LAE) and diffusion process. The LAE encodes and reconstructs LoRA weights. In the diffusion process, features extracted by the face and image encoder are combined with the Mixed Image Features (MIF) mechanism, and the resulting noisy latent is processed by a diffusion transformer to predict denoised latent. During inference, random noise and reference images are fed into DiffLoRA to generate LoRA weights.

cessitating a flattening operation. To maximize the preservation of structural information in the latent space, we flatten LoRA-B directly and flip LoRA-A to obtain a shape of  $\mathbb{R}^{n\times r}$  before flattening it. The resulting one-dimensional vectors are concatenated to form the input to the LAE. We then employ 1D convolutional layers as the primary compression layers to capture the structural feature of the LoRA weights.

Concerning the informational features of LoRA weights, we conducted an in-depth analysis of the impact of different magnitudes of LoRA parameters on the final generated images. We sorted the parameters in LoRA by their magnitude and divided them into four proportional groups: the first group representing the large weights and the last group representing the small weights. Subsequently, we either set the large weights and small weights to zero or perturb them with proportionally scaled noise. As illustrated in Figure 4, perturbing or zeroing small weights has little effect on the generated images, while doing the same to large weights significantly degrades the identity fidelity of the images.

This analysis reveals that larger LoRA weights tend to encapsulate more precise information about specific identity. Consequently, to enhance the reconstruction of larger weights during the compression and reconstruction process, we propose a novel loss function termed the weight-preserved loss for training the LAE. The weight-preserved



Figure 4: An example demonstrating the impact of perturbing or zeroing LoRA weights on generated images.

loss is incorporated into the original reconstruction loss and specifically targets the larger weights. The implementation of the weight-preserved loss in our LAE is given by the following formula:

$$\mathcal{L}_{WP} = \frac{1}{n} \sum_{i=1}^{n} |x_i| \cdot |x_i - \hat{x}_i|, \qquad (2)$$

where n is the number of parameters,  $x_i$  represents the i-th parameter, and  $\hat{x}_i$  represents the i-th reconstructed parame-

ter. The term  $|x_i| \cdot |x_i - \hat{x}_i|$  emphasizes the reconstruction error for larger weights. By integrating the weight-preserved loss into the training process, our approach ensures a more accurate preservation of critical information encoded in the larger weights, thereby significantly improving the quality of generated images post-reconstruction. Moreover, our LAE can compress the original LoRA weights by nearly 300 times, demonstrating an exceptional compression and reconstruction performance.

Mixed Image Features. The core concept of MIF is to leverage both facial details and general image information to better extract identity features, thereby improving the accuracy of the denoising process. Drawing inspiration from Mixture-of-Experts (MoE) structure (Shazeer et al. 2016), MIF combines image features and face features with a gate network. The overall workflow is illustrated in Figure 5.

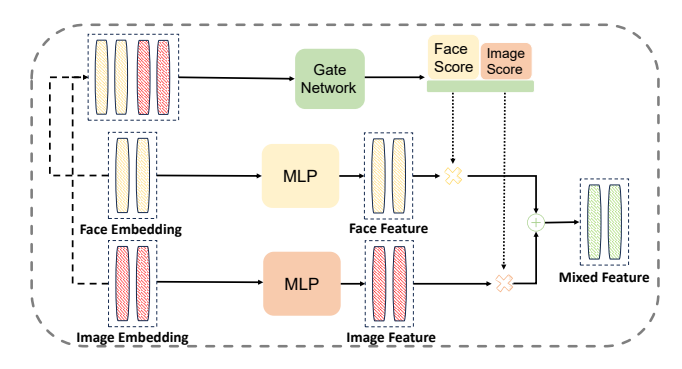


Figure 5: MIF mechanism. Our MIF consists of a MOE-inspired gate network to combine face embedding  $E_{face}$  and image embedding  $E_{img}$  into mixed features for improved identity feature extraction.

We first obtain the face embedding containing facial details for identity recognition from the Face Encoder  $(E_f)$  and the image embedding including background and overall appearance from the Image Encoder  $(E_{img})$  based on the reference image, and the concatenate these embeddings to obtain the mixed embedding.

By passing the mixed embedding to the Gate Network (G), we can obtain the Face Score  $(S_f)$  represents the importance of facial features, while the Image Score  $(S_i)$  represents the importance of general image features. And the mixed features can be calculated based on the scores. The forward process of MIF can be represented as:

$$\mathbf{h} = S_{\mathrm{img}} \odot \mathrm{MLP}(E_{\mathrm{img}}(I)) + S_{\mathrm{face}} \odot \mathrm{MLP}(E_{\mathrm{face}}(I)),$$
 (3) where  $S_{img}, S_{face} = \mathrm{Gate}(Z) = \mathrm{Softmax}(f(Z))$  and  $Z$  represent the mixed embedding. Here,  $\odot$  denotes scalar multiplication, and the function  $f$  can be a simple linear layer. **Denoising Process.** Transformers have demonstrated exceptional capabilities in handling long sequences in the language domain, making them an ideal choice for modeling the LoRA latent representations (Erkoç et al. 2023). Our diffusion model, based on the DiT architecture, is designed to process LoRA latent representations with noise added and subsequently predict the original latent representations. Additionally, we utilize Adaptive Layer Normaliza-

tion (AdaLN) mechanisms to incorporate mixed features to guide the diffusion process.

During diffusion modeling, we optimize the parameters  $\theta$  of our model  $M_{\theta}$  to minimize the mean squared error (MSE) loss:

$$L(\theta) = \mathbb{E}_{t,x_0,c} \left[ w_t \left\| M_{\theta}(\alpha_t x_0 + \sigma_t \epsilon, t, c) - x_0 \right\|^2 \right], \quad (4)$$

here,  $M_{\theta}$  denotes the DiT architecture model parameterized by  $\theta$ , t is a time step uniformly sampled from the range [0,T], and  $\epsilon$  is standard Gaussian noise. The parameters  $\alpha_t$ ,  $\sigma_t$ , and  $w_t$  are diffusion noise parameters. The term  $x_0$  represents the latent representations, summed with the positional encoding vector, while c denotes the condition integrated into the diffusion model through MIF.

We illustrate the inference process for LoRA weights in Figure 3. Random noise is denoised to the LoRA latent representations guided by the reference image. We employ DDIM (Song, Meng, and Ermon 2020) to sample new LoRA weights during the diffusion process.

## **LoRA Weight Pipeline**

As illustrated in Figure 6, we develop the pipeline for generating the high-quality LoRA weight dataset. Our approach begins with collecting facial images from the FFHQ (Karras, Laine, and Aila 2019) and CelebA-HQ (Karras et al. 2018) datasets. To ensure the performance of LoRA weights, we utilize PhotoMaker (Li et al. 2024) to generate 100 distinct images for each individual at the resolution of 1024×1024. Through this pipeline, we create a diverse image dataset suitable for training and deriving 100k LoRA weights.



Figure 6: Pipeline for constructing LoRA weight dataset.

**Image Collection.** We begin by obtaining high-quality facial images from the FFHQ (Karras, Laine, and Aila 2019) and CelebA-HQ (Karras et al. 2018) datasets, which serve as the basis for our pipeline.

**Image Generation.** Utilizing the PhotoMaker(Li et al. 2024), we can generate 100 diverse images for each individual with 100 unique prompts that capture a wide range of perspectives, gestures, and aesthetics. The prompts were specifically crafted for male and female categories, to create a comprehensive and diverse dataset. This step ensures a diverse set of images representing various expressions, attributes, and scenes for each identity.

Image Filtering and Preprocessing. We employ Insight-Face to calculate the facial similarity between the generated images and the original image. The top 85 images with the highest similarity scores are selected. These selected images are enriched and undergo further preprocessing, including cropping, flipping, and color transformation through various data augmentation operations.



Figure 7: Comparisons with several baseline methods. DiffLoRA consistently outperforms other methods by producing images with higher diversity and enhanced realism, while preserving identity fidelity.

**Training with DreamBooth.** The preprocessed 85 images are then used to train the SDXL model with the DreamBooth method (Ruiz et al. 2023).

## **Experiments**

### **Training Details**

The encoder of LAE employs multiple 1D convolution kernels, sized to match the rank of the LoRA weights, to compress the weight vectors into a lower-dimensional vector. Attention layers and residual connections are integrated into the encoder to enhance its performance. The decoder uses attention layers combined with an MLP for reconstructing the compressed weights. The LAE optimization process is performed using AdamW on 4 NVIDIA 3090 GPUs for about a week, with a batch size of 4 and a learning rate of 2e-5. In the diffusion phase, we trained a 16-layer, 1454-dimension DiT model. During training, images of the same identity are randomly sampled as conditions to create mixed image features. We use AdamW with a batch size of 32 and a learning rate of 1e-4, implementing 1000 diffusion timesteps with a linear noise scheduler ranging from 0.0001 to 0.012.

#### **Evaluation Metrics**

Following DreamBooth (Ruiz et al. 2023), we use the DINO (Caron et al. 2021) and CLIP-I (Gal et al. 2023) metrics to measure identity fidelity, and the CLIP-T metric to assess text-image consistency. However, since the CLIP-T metric may not fully capture the nuances of text-image alignment, we also compute the Image Reward score (Xu et al. 2024) to further evaluate the alignment and quality of the generated images concerning the text prompts. To further evaluate

identity fidelity, we measure the face embedding similarity, referred to as Face Sim, extracted by the InsightFace model between the generated and reference images. The quality of the generated images is assessed using the FID metric, which compares the distribution of generated images with those from MS-COCO, where lower FID values indicate better image quality. We assess the inference cost by evaluating personalization speed based on whether the method involves tuning or is tuning-free. For tuning-free methods, only inference time is measured, whereas for methods requiring tuning, both training and inference times are included. Personalization speed is measured on a single NVIDIA A6000 GPU.

#### **Evaluation Dataset**

Our evaluation dataset consists of 25 identities, comprising 10 male and 15 female identities, each represented by images that are not included in the training set. This setup is intended to assess the model's generalization ability. Additionally, we have prepared 30 prompts, encompassing simple, complex, and multi-angle prompts to ensure a comprehensive evaluation. For each prompt corresponding to each identity, we generate 4 images for evaluation.

#### **Comparisons**

**Qualitative Comparisons.** To evaluate the performance of DiffLoRA, we conducted a comparative analysis with LoRA-DreamBooth, Textual Inversion, InstantID, and PhotoMaker. We employed the default hyperparameters as proposed in their respective works, except for LoRA-DreamBooth, which was configured to align with our LoRA dataset pipeline. Unlike other methods that tend to overfit

Model	Image Reward↑	DINO↑(%)	CLIP-I↑(%)	CLIP-T↑(%)	Face Sim↑(%)	FID↓	Speed↓(s)
LoRA-DreamBooth	1.44	45.4	67.0	30.7	35.4	437.5	1260
Textual Inversion	1.10	31.2	67.6	30.6	31.6	451.0	810
InstantID	0.41	40.8	67.7	29.0	40.0	448.3	42
PhotoMaker	1.31	33.5	66.7	31.5	23.4	447.0	34
DiffLoRA (Ours)	1.46	47.4	68.3	30.6	42.2	436.7	28

Table 1: We compare our method with several baselines in terms of identity fidelity (DINO, CLIP-I, Face Sim), text-image consistency (CLIP-T, Image Reward), image quality (FID), and inference cost (personalization speed).



**Prompt: A man wearing a suit and tie**Figure 8: Visualization of generated results under different settings.

Method	Face Sim↑(%)	DINO↑(%)	CLIP I↑(%)
No Face Feature	22.45	44.95	61.28
No Image Feature	40.24	45.66	63.09
No WP Loss	37.31	47.23	59.77
Ours $(N=1)$	42.24	47.41	68.35
Ours $(N=2)$	42.74	47.33	65.40
Ours $(N=4)$	42.48	48.02	65.36
Ours $(N=6)$	42.90	48.39	64.20

Table 2: Ablation studies on identity fidelity metric (Face Sim, DINO), text-image consistency metrics (CLIP T).

to the reference image or compromise the identity fidelity, DiffLoRA consistently outperforms these methods by producing images with higher diversity and enhanced realism. **Quantitative Comparisons.** In our quantitative experiments, the effectiveness and efficiency of DiffLora were evaluated using multiple metrics covering various aspects: text-image consistency, identity fidelity, generation quality, and personalization speed. As illustrated in Table 2, our method achieved the highest scores across almost all metrics. The results demonstrate that our method satisfies the requirements for generating high-quality images with a high level of identity fidelity, as evidenced by achieving the highest CLIP-I, DINO scores, and Face Sim. Additionally, Difflora exhibited the lowest inference cost, as reflected in the personalization speed, compared to other methods.

#### **Ablation Studies**

As illustrated in Table 2 and Figure 8, our analysis reveals the impact of different components of the DiffLoRA method on the quality of generated images.

**Impact of the Mixed Image Features (MIF).** When the gate network in MIF is removed from the process, using only face features (No Image Feature) or only image features (No Face Feature) for inference, there is a significant decrease in the identity preservation of the generated images. This drastic drop suggests that MIF plays a crucial role in guiding

DiffLoRA to generate accurate LoRA weights. Especially, only with image feature, the fundamental features of personalized generation are almost lost.

Impact of the Weight-Preserved Loss. We trained the LAE model without the Weight Preserved Loss (No WP Loss), which resulted in a noticeable decline in image quality. The generated faces were less similar to the input faces compared to when the WP loss was incorporated. Including the Weight Preserved Loss significantly improves the LAE's ability to reconstruct high-quality LoRA parameters. Consequently, this enhancement boosts the Face Sim from 37.1 to 42.2.

Impact of the number of reference images. Adjusting the number of reference images (N) during inference impacts identity fidelity and facial similarity. By averaging the embeddings of multiple reference images, we find that increasing the number of images improves facial similarity metrics but reduces the CLIP I metric. This indicates a trade-off between capturing detailed features and maintaining generalization, which is crucial for generating images that are both personalized and diverse.

### Conclusion

In this work, we have presented DiffLoRA, a novel method for human-centric personalized image generation. Our approach employs a latent diffusion-based hypernetwork framework to predict LoRA weights for specific identity adaptation in the SDXL, enabling tuning-free generation of high-fidelity portraits without extra inference cost. Experimental results show that DiffLoRA outperforms existing methods in text-image consistency, identity fidelity, generation quality, and inference efficiency. Overall, we believe DiffLoRA is the first to utilize diffusion models for LoRA weights generation, paving the way for more adaptive frameworks in diverse architectures.

#### References

Avrahami, O.; Aberman, K.; Fried, O.; Cohen-Or, D.; and Lischinski, D. 2023. Break-a-scene: Extracting multiple

- concepts from a single image. In SIGGRAPH Asia 2023 Conference Papers, 1–12.
- Biderman, D.; Ortiz, J. G.; Portes, J.; Paul, M.; Greengard, P.; Jennings, C.; King, D.; Havens, S.; Chiley, V.; Frankle, J.; et al. 2024. Lora learns less and forgets less. *arXiv preprint arXiv:2405.09673*.
- Caron, M.; Touvron, H.; Misra, I.; Jégou, H.; Mairal, J.; Bojanowski, P.; and Joulin, A. 2021. Emerging properties in self-supervised vision transformers. In *Proceedings of the IEEE/CVF international conference on computer vision*, 9650–9660.
- Cui, S.; Guo, J.; An, X.; Deng, J.; Zhao, Y.; Wei, X.; and Feng, Z. 2024. IDAdapter: Learning Mixed Features for Tuning-Free Personalization of Text-to-Image Models. In *Proceedings of the IEEE/CVF Conference on Computer Vision and Pattern Recognition*, 950–959.
- Erkoç, Z.; Ma, F.; Shan, Q.; Nießner, M.; and Dai, A. 2023. Hyperdiffusion: Generating implicit neural fields with weight-space diffusion. In *Proceedings of the IEEE/CVF international conference on computer vision*, 14300–14310.
- Gal, R.; Alaluf, Y.; Atzmon, Y.; Patashnik, O.; Bermano, A. H.; Chechik, G.; and Cohen-or, D. 2023. An Image is Worth One Word: Personalizing Text-to-Image Generation using Textual Inversion. In *The Eleventh International Conference on Learning Representations*.
- Guo, Q.; Zhang, C.; Zhang, Y.; and Liu, H. 2015. An efficient SVD-based method for image denoising. *IEEE transactions on Circuits and Systems for Video Technology*, 26(5): 868–880.
- Ha, D.; Dai, A. M.; and Le, Q. V. 2022. HyperNetworks. In *International Conference on Learning Representations*.
- Ho, J.; Jain, A.; and Abbeel, P. 2020. Denoising diffusion probabilistic models. *Advances in neural information processing systems*, 33: 6840–6851.
- Hore, A.; and Ziou, D. 2010. Image quality metrics: PSNR vs. SSIM. In 2010 20th international conference on pattern recognition, 2366–2369. IEEE.
- Hu, E. J.; Wallis, P.; Allen-Zhu, Z.; Li, Y.; Wang, S.; Wang, L.; Chen, W.; et al. 2022. LoRA: Low-Rank Adaptation of Large Language Models. In *International Conference on Learning Representations*.
- Ju, X.; Zeng, A.; Zhao, C.; Wang, J.; Zhang, L.; and Xu, Q. 2023. Humansd: A native skeleton-guided diffusion model for human image generation. In *Proceedings of the IEEE/CVF International Conference on Computer Vision*, 15988–15998.
- Karras, T.; Aila, T.; Laine, S.; and Lehtinen, J. 2018. Progressive Growing of GANs for Improved Quality, Stability, and Variation. In *International Conference on Learning Representations*.
- Karras, T.; Laine, S.; and Aila, T. 2019. A style-based generator architecture for generative adversarial networks. In *Proceedings of the IEEE/CVF conference on computer vision and pattern recognition*, 4401–4410.
- Kingma, D. P.; and Welling, M. 2013. Auto-encoding variational bayes. *arXiv preprint arXiv:1312.6114*.

- Klema, V.; and Laub, A. 1980. The singular value decomposition: Its computation and some applications. *IEEE Transactions on automatic control*, 25(2): 164–176.
- Kumari, N.; Zhang, B.; Zhang, R.; Shechtman, E.; and Zhu, J.-Y. 2023. Multi-concept customization of text-to-image diffusion. In *Proceedings of the IEEE/CVF Conference on Computer Vision and Pattern Recognition*, 1931–1941.
- Li, Z.; Cao, M.; Wang, X.; Qi, Z.; Cheng, M.-M.; and Shan, Y. 2024. Photomaker: Customizing realistic human photos via stacked id embedding. In *Proceedings of the IEEE/CVF Conference on Computer Vision and Pattern Recognition*, 8640–8650.
- Liu, X.; Ren, J.; Siarohin, A.; Skorokhodov, I.; Li, Y.; Lin, D.; Liu, X.; Liu, Z.; and Tulyakov, S. 2024. HyperHuman: Hyper-Realistic Human Generation with Latent Structural Diffusion. In *The Twelfth International Conference on Learning Representations*.
- Nichol, A. Q.; and Dhariwal, P. 2021. Improved denoising diffusion probabilistic models. In *International conference on machine learning*, 8162–8171. PMLR.
- Peebles, W.; Radosavovic, I.; Brooks, T.; Efros, A. A.; and Malik, J. 2022. Learning to learn with generative models of neural network checkpoints. *arXiv preprint arXiv*:2209.12892.
- Podell, D.; English, Z.; Lacey, K.; Blattmann, A.; Dockhorn, T.; Müller, J.; Penna, J.; and Rombach, R. 2023. Sdxl: Improving latent diffusion models for high-resolution image synthesis. *arXiv preprint arXiv:2307.01952*.
- Prasantha, H.; Shashidhara, H.; and Murthy, K. B. 2007. Image compression using SVD. In *International conference on computational intelligence and multimedia applications (ICCIMA 2007)*, volume 3, 143–145. IEEE.
- Radford, A.; Kim, J. W.; Hallacy, C.; Ramesh, A.; Goh, G.; Agarwal, S.; Sastry, G.; Askell, A.; Mishkin, P.; Clark, J.; et al. 2021. Learning transferable visual models from natural language supervision. In *International conference on machine learning*, 8748–8763. PMLR.
- Ramesh, A.; Dhariwal, P.; Nichol, A.; Chu, C.; and Chen, M. 2022. Hierarchical text-conditional image generation with clip latents. *arXiv preprint arXiv:2204.06125*, 1(2): 3.
- Razavi, A.; Van den Oord, A.; and Vinyals, O. 2019. Generating diverse high-fidelity images with vq-vae-2. *Advances in neural information processing systems*, 32.
- Ren, Y.; Fan, X.; Li, G.; Liu, S.; and Li, T. H. 2022. Neural texture extraction and distribution for controllable person image synthesis. In *Proceedings of the IEEE/CVF conference on computer vision and pattern recognition*, 13535–13544.
- Rombach, R.; Blattmann, A.; Lorenz, D.; Esser, P.; and Ommer, B. 2022. High-resolution image synthesis with latent diffusion models. In *Proceedings of the IEEE/CVF conference on computer vision and pattern recognition*, 10684–10695.
- Ruan, L.; Ma, Y.; Yang, H.; He, H.; Liu, B.; Fu, J.; Yuan, N. J.; Jin, Q.; and Guo, B. 2023. Mm-diffusion: Learning

- multi-modal diffusion models for joint audio and video generation. In *Proceedings of the IEEE/CVF Conference on Computer Vision and Pattern Recognition*, 10219–10228.
- Ruiz, N.; Li, Y.; Jampani, V.; Pritch, Y.; Rubinstein, M.; and Aberman, K. 2023. Dreambooth: Fine tuning text-to-image diffusion models for subject-driven generation. In *Proceedings of the IEEE/CVF conference on computer vision and pattern recognition*, 22500–22510.
- Ruiz, N.; Li, Y.; Jampani, V.; Wei, W.; Hou, T.; Pritch, Y.; Wadhwa, N.; Rubinstein, M.; and Aberman, K. 2024. Hyperdreambooth: Hypernetworks for fast personalization of text-to-image models. In *Proceedings of the IEEE/CVF Conference on Computer Vision and Pattern Recognition*, 6527–6536.
- Saharia, C.; Chan, W.; Saxena, S.; Li, L.; Whang, J.; Denton, E. L.; Ghasemipour, K.; Gontijo Lopes, R.; Karagol Ayan, B.; Salimans, T.; et al. 2022. Photorealistic text-to-image diffusion models with deep language understanding. *Advances in neural information processing systems*, 35: 36479–36494.
- Shazeer, N.; Mirhoseini, A.; Maziarz, K.; Davis, A.; Le, Q.; Hinton, G.; and Dean, J. 2016. Outrageously Large Neural Networks: The Sparsely-Gated Mixture-of-Experts Layer. In *International Conference on Learning Representations*.
- Sohl-Dickstein, J.; Weiss, E.; Maheswaranathan, N.; and Ganguli, S. 2015. Deep unsupervised learning using nonequilibrium thermodynamics. In *International conference on machine learning*, 2256–2265. PMLR.
- Song, J.; Meng, C.; and Ermon, S. 2020. Denoising diffusion implicit models. *arXiv preprint arXiv:2010.02502*.
- Tewel, Y.; Gal, R.; Chechik, G.; and Atzmon, Y. 2023. Keylocked rank one editing for text-to-image personalization. In *ACM SIGGRAPH 2023 Conference Proceedings*, 1–11.
- Valevski, D.; Lumen, D.; Matias, Y.; and Leviathan, Y. 2023. Face0: Instantaneously conditioning a text-to-image model on a face. In *SIGGRAPH Asia 2023 Conference Papers*, 1–10.
- Wang, B.; Zheng, H.; Liang, X.; Chen, Y.; Lin, L.; and Yang, M. 2018. Toward characteristic-preserving image-based virtual try-on network. In *Proceedings of the European conference on computer vision (ECCV)*, 589–604.
- Wang, K.; Xu, Z.; Zhou, Y.; Zang, Z.; Darrell, T.; Liu, Z.; and You, Y. 2024a. Neural network diffusion. *arXiv* preprint *arXiv*:2402.13144.
- Wang, Q.; Bai, X.; Wang, H.; Qin, Z.; and Chen, A. 2024b. Instantid: Zero-shot identity-preserving generation in seconds. *arXiv preprint arXiv:2401.07519*.
- Wei, Y.; Zhang, Y.; Ji, Z.; Bai, J.; Zhang, L.; and Zuo, W. 2023. Elite: Encoding visual concepts into textual embeddings for customized text-to-image generation. In *Proceedings of the IEEE/CVF International Conference on Computer Vision*, 15943–15953.
- Xiao, G.; Yin, T.; Freeman, W. T.; Durand, F.; and Han, S. 2023. Fastcomposer: Tuning-free multi-subject image generation with localized attention. *arXiv* preprint *arXiv*:2305.10431.

- Xu, J.; Liu, X.; Wu, Y.; Tong, Y.; Li, Q.; Ding, M.; Tang, J.; and Dong, Y. 2024. Imagereward: Learning and evaluating human preferences for text-to-image generation. *Advances in Neural Information Processing Systems*, 36.
- Ye, H.; Zhang, J.; Liu, S.; Han, X.; and Yang, W. 2023. Ipadapter: Text compatible image prompt adapter for text-to-image diffusion models. *arXiv preprint arXiv:2308.06721*.
- Zeng, Y.; Patel, V. M.; Wang, H.; Huang, X.; Wang, T.-C.; Liu, M.-Y.; and Balaji, Y. 2024. JeDi: Joint-Image Diffusion Models for Finetuning-Free Personalized Text-to-Image Generation. In *Proceedings of the IEEE/CVF Conference on Computer Vision and Pattern Recognition*, 6786–6795.
- Zhang, B.; Luo, C.; Yu, D.; Li, X.; Lin, H.; Ye, Y.; and Zhang, B. 2024. Metadiff: Meta-learning with conditional diffusion for few-shot learning. In *Proceedings of the AAAI Conference on Artificial Intelligence*, 15, 16687–16695.
- Zhang, W.; Cun, X.; Wang, X.; Zhang, Y.; Shen, X.; Guo, Y.; Shan, Y.; and Wang, F. 2023. Sadtalker: Learning realistic 3d motion coefficients for stylized audio-driven single image talking face animation. In *Proceedings of the IEEE/CVF Conference on Computer Vision and Pattern Recognition*, 8652–8661.
- Zhou, X.; Yin, M.; Chen, X.; Sun, L.; Gao, C.; and Li, Q. 2022. Cross attention based style distribution for controllable person image synthesis. In *European Conference on Computer Vision*, 161–178. Springer.